

Analytic eigenvalue structure of the 1+1 Dirac oscillator

Bo-Xing Cao and Fu-Lin Zhang*

Department of Physics, School of Science, Tianjin University, Tianjin 300072, China

(Dated: October 11, 2019)

We study the analytic structure for eigenvalues of the one-dimensional Dirac oscillator, by analytically continuing its frequency on the complex plane. A twofold Riemann surface is found connecting the two states of a pair of particle and antiparticle. One can, at least in principle, accomplish the transition from a positive energy state to its antiparticle state, by moving the frequency continuously on the complex plane, without changing the Hamiltonian after transition. This result provides a visual explanation for the absence of a negative energy state with the quantum number $n = 0$.

Keywords:

I. INTRODUCTION

Experimental studies of exceptional points in several systems [1–5] make the functions of a complex variable being no longer limited to an abstract tool in physics. On the other hand, very recently, the theoretical research on the structure of the Riemann surface has been extended to a coupled quantum system, and unexpected behaviors have been found [6, 7]. Namely, in the system of two coupled harmonic oscillators, there exists an eightfold Riemann surface structure of eigenvalues as functions of the complex coupling parameter, which collapses to a fourfold one in the case of the ground state. By analytically continuing the system through the Riemann surface and finally returning to the decoupling limit, one can access the unconventional phases of both oscillators, which are originally found in the analytic continuation of the frequencies [8].

In this work, we study the Dirac oscillator [9, 10] in one spatial dimension. The motivation for this research is not only to extend the study on the harmonic oscillator to its relativistic version, but also based on the following considerations. On the one hand, the one-dimensional Dirac oscillator can be derived by linearizing the quadratic form $E^2 = m^2 + p^2 + m^2\omega^2x^2 - \beta m\omega$, as Dirac's original approach to propose his equation [11], with ω being the frequency and β being one of the Dirac matrices. Hence, it naturally has the property of a square root, which is a key cause of the structure of Riemann surface in the non-relativistic harmonic systems [6–8]. On the other hand, it can be regarded as a coupled quantum system composed by a harmonic oscillator and a spin. It is interesting to re-examine the Riemann surface when one of the harmonic oscillators in the model studied in [6, 7] is replaced by a spin.

The Dirac oscillator [9, 10] is obtained from the free Dirac equation by the substitution $\mathbf{p} \rightarrow \mathbf{p} - i\beta m\omega\mathbf{x}$, which has become the paradigm for the construction of covariant quantum models with some well determined nonrelativistic limit [12]. It exhibits abundant alge-

braic properties [13–17], and is used in various branches of physics, such as nuclear physics [18] and subnuclear physics [19]. Recently, there has been a growing interest in simulating the Dirac oscillator in other physical systems, such as quantum optics [20–23] and classical microwave setups [12, 24]. The experimental progresses on simulating the Dirac oscillator [12, 24] and observing exceptional points [1–3] in microwave setups, make it possible to experimentally observe the Riemann surface studied in the present work.

By analytically continuing the frequency of the one-dimensional Dirac oscillator on the complex plane, an unconventional spectrum arises accompanied with the conventional spectrum. Such characteristic is inherited from the nonrelativistic harmonic oscillator. However, the difference is that, the conventional states and unconventional states of the Dirac oscillator locate on different Riemann surfaces. Namely, although the four eigenvalues with the same quantum number n can be expressed as a nested square-root function, the absence of a symmetry of $\omega \rightarrow -\omega$ in the Dirac oscillator leads to that, the eigenfunction with a negative frequency no longer belongs to the system. Hence, the two conventional eigenvalues, of a particle and its antiparticle, should be considered to belong to two sheets of a square-root function of the frequency parameter ω . And, the two unconventional eigenvalues belongs to another square-root function. On the twofold Riemann surface, one can move the Dirac oscillator from a positive energy state to its antiparticle state, by moving the system through a branch cut on the complex-frequency plane. From this angle of view, the disappearance of the branch point provides an interpretation for the absence of negative energy state with $n = 0$.

In the following section, we review the analytic structure of one-dimensional harmonic oscillator. Further, based on these results, the Dirac oscillator is studied in detail. And finally, we give a brief summary.

II. HARMONIC OSCILLATOR

Let us begin with the nonrelativistic harmonic oscillator, whose analytical properties have been discussed in

*Corresponding author: flzhang@tju.edu.cn

[6–8]. We give its eigenfunctions in both the conventional and unconventional spectra, based on which one can solve the eigenvalue problem for the relativistic case concisely. The Hamiltonian of a nonrelativistic harmonic oscillator is given by

$$H = \frac{1}{2m}p^2 + \frac{1}{2}m\omega^2x^2. \quad (1)$$

In this work, we set the reduced Planck constant $\hbar = 1$. In the asymptotic region $|x| \rightarrow +\infty$, $m\omega^2x^2 \gg E$, the stationary Schrödinger equation reads

$$\phi'' = m^2\omega^2x^2\phi. \quad (2)$$

Its approximate solutions can be written as

$$\phi = e^{f(x)}, \quad (3)$$

in which $f(x) = \pm\frac{1}{2}m\omega x^2$ is derived from

$$[f'(x)]^2 = m^2\omega^2x^2. \quad (4)$$

Making the substitutions $\xi = \sqrt{m\omega}x$, $k = 2E/\omega$ and $\phi(\xi) = h(\xi)e^{\mp\xi^2/2}$, one obtains

$$\frac{d^2h}{d\xi^2} \mp 2\xi\frac{dh}{d\xi} + (k \mp 1)h = 0. \quad (5)$$

It is the defining differential equation for the Hermite polynomials if $k = \pm(2n + 1)$ and $n = 0, 1, 2, \dots$, which can be represented as

$$h_{\pm n}(\xi) = (\pm 1)^n e^{\mp\xi^2} \frac{\partial^n}{\partial \xi^n} e^{\pm\xi^2}. \quad (6)$$

The plus sign corresponds to the conventional Hermite polynomials, $H_n(\xi) = h_{+n}(\xi)$, and the consequently conventional eigenfunctions of harmonic oscillator. We denote the ones with minus sign as $h_{-n}(\xi)$, which leads to nonnormalizable unconventional eigenfunctions [6]. Then, the eigenvalues and corresponding eigenfunctions are

$$E_n^\pm = \pm(n + \frac{1}{2})\omega, \quad \phi_n^\pm(\xi) = h_{\pm n}(\xi)e^{\mp\frac{1}{2}\xi^2}. \quad (7)$$

Obviously, the \pm signs in the above results come from the square root of Eq. (4). Consequently, the eigenvalues with the same quantum number n are merely different branches of a multivalued function of complex ω , which can be written as

$$E_n(\omega) = \pm(n + \frac{1}{2})\sqrt{\omega^2} = (n + \frac{1}{2})e^{\frac{1}{2}Ln(\omega^2)}. \quad (8)$$

With the aid of the logarithmic function in above expression, one can easily notice the connection structure of the function.

In Fig. 1, we show the real part of the Riemann surface for $n = 0$. The function is unchanged under $\omega \rightarrow -\omega$,

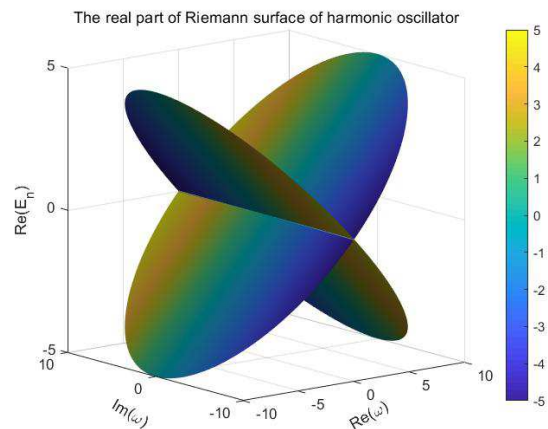


FIG. 1: (Color online) The real part of the Riemann surface for one-dimensional harmonic oscillator with the quantum number $n = 0$. The imaginary part is shown by color.

which can be traced back to the symmetry of the Hamiltonian (1). However, the eigenvalues change sign, as the argument of ω runs continuously from 0 to π . There are two coalescing branch points at $\omega = 0$, and the two associated branch cuts can be chosen along the imaginary ω axis. Each additional π on the argument of ω moves the system from one branch to another, and changes the sign of eigenvalues though the Hamiltonian remains unchanged. Simultaneously, the variable ξ is changed into $i\xi$, which leads to

$$\phi_n^+(\xi) \rightarrow \phi_n^+(i\xi) = -i^n \phi_n^-(\xi). \quad (9)$$

That is, by such analytic continuation, we reach an unconventional state, starting from a conventional one. A similar process can move the system from an unconventional state to a conventional one.

III. DIRAC OSCILLATOR

A. Spectra

In this part, we study the one-dimensional version of the Dirac oscillator, whose Hamiltonian is given by

$$\mathcal{H} = \alpha(p - i\beta m\omega x) + \beta m, \quad (10)$$

where ω is a natural frequency, α and β are the Dirac matrices, and the light velocity is set to $c = 1$. We set the frequency ω to be positive real in this subsection. The Dirac matrices are conveniently defined in terms of the Pauli matrices

$$\alpha = \sigma_y, \quad \beta = \sigma_z. \quad (11)$$

It is instructive to square the Hamiltonian (10)

To observe its relation with the nonrelativistic harmonic oscillator, one can square the Hamiltonian (10) and obtain

$$\mathcal{H}^2 = m^2 + p^2 + m^2\omega^2 x^2 - \sigma_z m\omega. \quad (12)$$

and consequently,

$$\frac{\mathcal{H}^2 - m^2}{2m} = \frac{p^2}{2m} + \frac{1}{2}m\omega^2 x^2 - \frac{1}{2}\sigma_z \omega. \quad (13)$$

In the nonrelativistic limit, $m \gg \omega$ and $\mathcal{H} \rightarrow m$, the kinetic energy $\mathcal{H} - m \rightarrow (\mathcal{H}^2 - m^2)/2m$. The Dirac oscillator becomes a decoupled system composed of a harmonic oscillator and a spin with a resonant frequency. In addition, the leading term of the relativistic correction is proportional to ω^2/m . Hence, the natural frequency ω also plays the role of a coupling constant. On the other hand, the relations in (12) and (13) enable one to solve the eigenvalue problem of \mathcal{H} based on the results of the harmonic oscillator. The process is as follows.

First, the eigenvalues and eigenfunctions of \mathcal{H}^2 can be obtained directly. Denoting the eigenenergies of the Dirac oscillator as \mathcal{E} , the eigenvalues of \mathcal{H}^2 are \mathcal{E}^2 . Corresponding to each solutions in (7), one can obtain

$$\mathcal{E}^2 = m^2 \pm 2nm\omega. \quad (14)$$

and the two-component eigenstates

$$\psi_n^+ = \begin{pmatrix} a_n^+ \phi_n^+(\xi) \\ b_n^+ \phi_{n-1}^+(\xi) \end{pmatrix}, \quad \psi_n^- = \begin{pmatrix} a_n^- \phi_{n-1}^-(\xi) \\ b_n^- \phi_n^-(\xi) \end{pmatrix}, \quad (15)$$

where we denote $\phi_{-1}^\pm(\xi) = \phi_0^\mp(\xi)$ and $\xi = \sqrt{m\omega}x$. And, a_n^\pm and b_n^\pm are free parameters, which is due to the double degenerate caused by the resonance between the spin and harmonic oscillator in (13). The states ψ_0^+ and ψ_0^- represent the same degenerate subspace.

Second, diagonalizing the Hamiltonian in the degenerate subspaces of \mathcal{H}^2 , one can find the eigenfunctions of \mathcal{H}

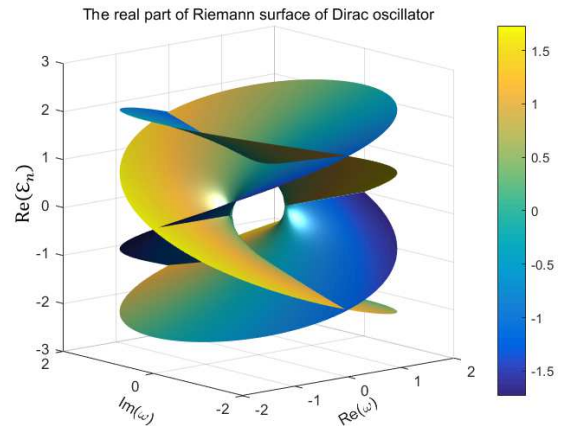
$$\Psi_{\pm n}^+ = \begin{pmatrix} (m \pm \sqrt{m^2 + 2nm\omega})\phi_n^+(\xi) \\ 2n\sqrt{m\omega}\phi_{n-1}^+(\xi) \end{pmatrix}, \quad (16)$$

$$\Psi_{\pm n}^- = \begin{pmatrix} 2n\sqrt{m\omega}\phi_{n-1}^-(\xi) \\ (m \mp \sqrt{m^2 - 2nm\omega})\phi_n^-(\xi) \end{pmatrix}, \quad (17)$$

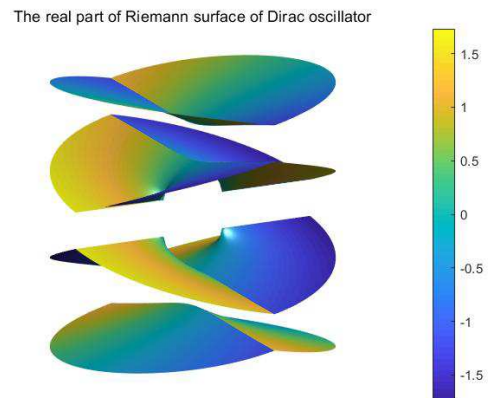
corresponding to the eigenvalues

$$\mathcal{E}_{\pm n}^\pm = \pm \sqrt{m^2 \pm 2nm\omega}, \quad (18)$$

where the subscripts indicate the signs before the square roots, and the superscripts indicate the ones in the square roots. When $n = 0$, Ψ_{-0}^+ and Ψ_{+0}^- vanish, and the eigenenergies $\mathcal{E}^\pm = \pm m$ corresponds to the states Ψ_{+0}^+ and Ψ_{-0}^- respectively. And the lower/upper component



(a)



(b)

FIG. 2: (Color online) (a) The real part of Riemann surface of $\mathcal{E}_n(\omega)$ with $m = 1$ and $n = 1$. Shapes of the four sheets of the function are shown in (b). The amount of imaginary part is shown by color.

in Ψ_{+0}^+/Ψ_{-0}^- is zero. These results indicate that, the conventional and unconventional states appear separately in $\Psi_{\pm n}^+$ and $\Psi_{\pm n}^-$. Hence, we refer to $\Psi_{\pm n}^-$ as the unconventional eigenfunctions of the Dirac oscillator, as $\Psi_{\pm n}^+$ are the conventional ones [25].

B. Analytic structure

We now analytically continue the frequency on the complex plane and examine the analytic structure of the Dirac oscillator. In this subsection, we show that, although the eigenvalue (18) with a fixed quantum number $n \neq 0$ can be expressed as a nested square-root function, the conventional states and unconventional states actually belong to two different square-root functions.

Since the the inner \pm signs (18) are from the square root to derive the eigenfunctions of the Harmonic oscil-

lator, it is naturally to rewrite the eigenvalue as a nested square-root function

$$\mathcal{E}_n(\omega) \equiv \pm \sqrt{m^2 \pm 2nm\sqrt{\omega^2}}. \quad (19)$$

It has six square-root branch points, four occurring at $\omega = 0$ and two at $\omega = \pm m/(2n)$. The associated branch cuts at $\omega = 0$ are chosen along the imaginary ω axis, and the ones at $\omega = \pm m/(2n)$ along the real ω axis. They connect four sheets of the Riemann surface pairwise to one another.

A visualization of this surface and its four sheets is shown in Fig. 2. Let us take a brief look at the function. We start from a positive real $\omega = |\omega| > m/(2n)$ and $\mathcal{E}_n(\omega) = \sqrt{m^2 + 2nm\sqrt{\omega^2}}$, which locates on the top sheet. Increasing the phase θ of $\omega = e^{i\theta}|\omega|$, one can enter the second sheet after pass through the positive-imaginary axis. Next, running θ to the region of $(\pi, 3\pi/2)$, one get the third sheet. Follow that, when ω reaches the fourth quadrant, $\mathcal{E}_n(\omega)$ enters its fourth sheet, where $\mathcal{E}_n(\omega) = -\sqrt{m^2 + 2nm\sqrt{\omega^2}}$ when $\theta = 2\pi$. If the phase θ continues to increase, the function reenters the third, second, and first sheets in turn. When $\theta = 4\pi$, $\mathcal{E}_n(\omega)$ gets back to the initial point.

An obvious feature of the above route is that, only a half of the Riemann surface is reached by smoothly moving the ω . Starting from a positive real ω , one goes through the first and fourth sheets with $\text{Re}(\omega) > 0$, and the second and third ones with $\text{Re}(\omega) < 0$. The four regions actually compose the Riemann surface of the two-valued function

$$\mathcal{E}_n^+(\omega) \equiv \pm \sqrt{m^2 + 2nm\omega}. \quad (20)$$

The start and end points of the above route are two eigenvalues of the initial Hamiltonian, corresponding to two conventional eigenstates. However, although the function on the negative-real axis equals two unconventional eigenvalues, the state reached by verifying the frequency in a conventional eigenstate from ω to $-\omega$ is no longer an eigenstate of the initial Hamiltonian. This difference with the Harmonic oscillator comes from the fact that the symmetry of $\omega \rightarrow -\omega$ is broken in the Dirac oscillator, which can be easily noticed by the linear terms in (12) and (13). Therefore, the Riemann surface of the two-valued function $\mathcal{E}_n^+(\omega)$ connects the two conventional states with the same quantum number n , and similarly one can find that the two-valued function

$$\mathcal{E}_n^-(\omega) \equiv \pm \sqrt{m^2 - 2nm\omega}. \quad (21)$$

connects the two unconventional states. And, starting from one of the conventional states in (16), it is impossible to reach an unconventional one of the same Hamiltonian by smoothly varying the frequency ω , and vice versa.

Based on the above considerations, the multi-value functions connecting the eigenvalues are $\mathcal{E}_n^+(\omega)$ and

$\mathcal{E}_n^-(\omega)$ rather than $\mathcal{E}_n(\omega)$. To show the connection structures, we take the conventional states for example. The results of the unconventional states can be easily obtained by simultaneously changing the two \pm signs in (18) and flipping the spin. The Riemann surface of $\mathcal{E}_n^+(\omega)$ is plotted in Fig. 3. It has one square-root branch point at $\omega = -m/(2n)$ when $n \neq 0$, and the associated branch cut can be chosen along the negative-real axis. Let the Dirac oscillator start from a positive energy state Ψ_{+n}^+ with $\mathcal{E}_n^+(\omega) = +\sqrt{m^2 + 2nm\omega}$, we run the argument θ of $\omega = e^{i\theta}|\omega|$ from 0 to 2π . When $|\omega| < m/(2n)$, the system gets back to the initial state Ψ_{+n}^+ . When $|\omega| > m/(2n)$, the system passes through the branch cut, and reaches its antiparticle state Ψ_{-n}^+ with a negative energy $\mathcal{E}_n^+(\omega) = -\sqrt{m^2 + 2nm\omega}$.

On the negative-real axis, the Hamiltonian in the degenerate subspaces of ψ_n^+ can be written as

$$\mathcal{H}_n^+ = \begin{pmatrix} m & i\sqrt{m|\omega|} \\ i2n\sqrt{m|\omega|} & -m \end{pmatrix}. \quad (22)$$

Under the similarity transformation, it is be equivalent to

$$\mathcal{H}_n^{+'} = \begin{pmatrix} i\sqrt{2nm|\omega|} & m \\ m & -i\sqrt{2nm|\omega|} \end{pmatrix}, \quad (23)$$

which is a special case of the 2×2 PT-symmetric matrix Hamiltonian studied in [26]. In the transition between a state to its antiparticle state, the system goes through a region of broken PT symmetry on the negative-real axis, as the eigenvalue becomes complex when $\theta = \pi$, which is also noticed in the system of two coupled harmonic oscillators [7]. The PT symmetry breaking can be regarded as a relativistic effect, as it requires a large enough *kinetic energy* that $2n|\omega| > m$. The lower bound of $|\omega|$ to break the PT symmetry increases with the quantum number n decreases. When $n = 0$, the bound becomes $+\infty$. This result provides a visual explanation for the absence of Ψ_{-0}^+ .

IV. SUMMARY

We study the analytic structure of eigenvalues of the Dirac oscillator in one spatial dimension. There exist four eigenfunctions corresponding to an oscillator quantum number n , two of which are conventional states for a pair of particle and antiparticle, and the other two are unconventional. The difference with the coupled-oscillator system [6, 7] is that, the conventional states and unconventional ones are separately connected by two distinct functions. Namely, the two conventional states with the same quantum number n are connected by a twofold Riemann surface, for the eigenvalues as a function of frequency on the complex plane. So are the two unconventional states. The system can be transitioned smoothly among the states by an analytic continuation in the fre-

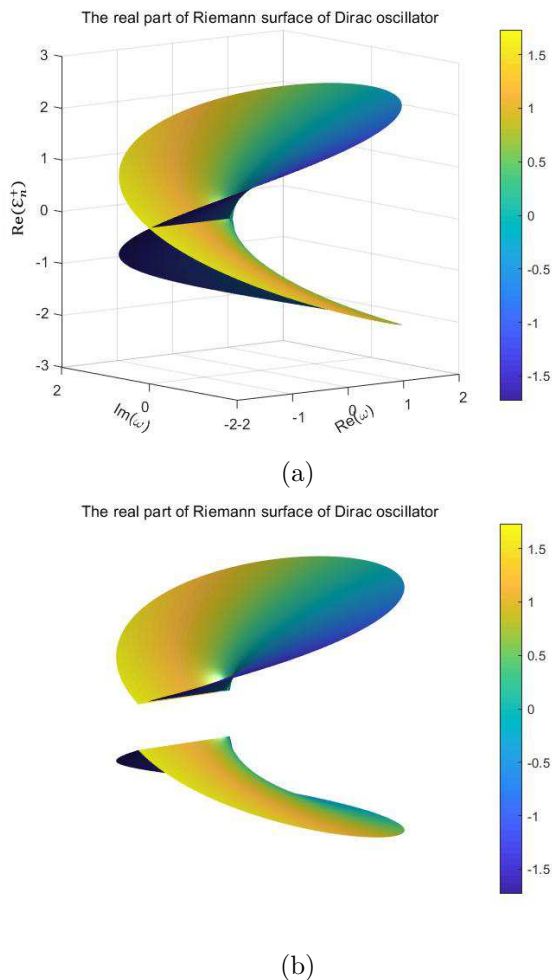


FIG. 3: (Color online) (a) The real part of Riemann surface of $\mathcal{E}_n^+(\omega)$ with $m = 1$ and $n = 1$. Shapes of the two sheets of the function are shown in (b). The amount of imaginary part is shown by color.

quency constant. The transition occurs at a region with sufficient relativistic effects, where the PT symmetry is broken on the negative real axis. Based on these results, the absence of a negative energy state with $n = 0$ can be intuitively explained by the disappearance of the branch point.

Further researches on this topic in several directions would be interesting. First, we look forward to an experimental verification of the analytic continuation studied in this work. Also, it is fascinating to consider the Berry phases [27] acquired by the system when it moves on the Riemann surfaces. Whether more elaborate structures arise from the Riemann surfaces in the two- or three-dimensional Dirac oscillators is also a natural question. Finally, could we give a physical meaning of the unconventional states? Or more specifically, whether the negative energy of an unconventional state in nonrelativistic harmonic oscillators [6–8] is a positive one actually, as the negative energy in the Dirac equation?

Acknowledgments

This work is supported by the NSF of China (Grant No. 11675119, No. 11575125 and No. 11105097). We thank Wu-Sheng Dai, Yun-Peng Liu and Wen-Ya Song for their discussions.

References

- [1] C. Dembowski, H.-D. Gräf, H. L. Heine, W. D. Heiss, H. Rehfeld, and A. Richter, Phys. Rev. Lett. **86**, 787 (2001).
- [2] B. Dietz, H. L. Harney, O. N. Kirillov, M. Miski-Oglu, A. Richter, and F. Schäfer, Phys. Rev. Lett. **106**, 150403 (2011).
- [3] J. Doppler, A. A. Mailybaev, J. Böhm, U. Kuhl, A. Girschik, F. Libisch, T. J. Milburn, P. Rabl, N. Moiseyev, and S. Rotter, Nature **537**, 76 (2016).
- [4] W. Chen, S. K. Özdemir, G. Zhao, J. Wiersig, and L. Yang, Nature **548**, 192 (2017).
- [5] H. Xu, D. Mason, L. Jiany, and J. G. E. Harris, Nature **537**, 80 (2016).
- [6] C. M. Bender, A. Felski, N. Hassanpour, S. P. Klevansky, and A. Beygi, Phys. Scr. **92**, 015201 (2017).
- [7] A. Felski and S. P. Klevansky, Phys. Rev. A **98**, 012127 (2018).
- [8] C. M. Bender and A. Turbiner, Phys. Lett. A **64**, 442 (1993).
- [9] M. Moshinsky and A. Szczepaniak, J. Phys. A: Math. Gen. **98**, 817 (1989).
- [10] E. Sadurní, AIP Conf. Proc. **1334**, 249 (2010).
- [11] P. A. M. Dirac, *The principles of quantum mechanics* (Oxford University Press 1930, 1965).
- [12] J. A. Franco-Villafañe, E. Sadurní, S. Barkhofen, U. Kuhl, F. Mortessagne, and T. H. Seligman, Phys. Rev. Lett. **111**, 170405 (2013).
- [13] O. L. de Lange, J. Phys. A: Math. Gen. **24**, 667 (1991).
- [14] J. Benitez, Phys. Rev. Lett. **64**, 1643 (1990).
- [15] C. Quesne and M. Moshinsky., J. Phys. A: Math. Gen. **23**, 2263 (1990).
- [16] R. Lisboa, M. Malheiro, A. S. de Castro, P. Alberto, and M. Fiolhais, Phys. Rev. C **69**, 024319 (2004).
- [17] F.-L. Zhang, B. Fu, and J.-L. Chen, Phys. Rev. A **80**, 054102 (2009).
- [18] J. Grineviciute and D. Halderson, Phys. Rev. C **85**, 054102 (2012).

- 054617 (2012).
- [19] E. Romera, Phys. Rev. A **84**, 052102 (2011).
- [20] A. Bermudez, M. A. Martin-Delgado, and E. Solano, Phys. Rev. A **76**, 041801 (2007).
- [21] A. Bermudez, M. A. Martin-Delgado, and E. Solano, Phys. Rev. Lett. **99**, 123602 (2007).
- [22] L. Lamata, J. León, T. Schätz, and E. Solano, Phys. Rev. Lett. **98**, 253005 (2007).
- [23] J. M. Torres, E. Sadurní, and T. H. Seligman, AIP Conf. Proc. **1323**, 301 (2010).
- [24] E. Sadurní, T. H. Seligman, and F. Mortessagne, New J. Phys. **12**, 053014 (2010).
- [25] R. Szmytkowski and M. Gruchowski, J. Phys. A: Math. Gen. **34**, 4991 (2001).
- [26] C. M. Bender, D. C. Brody, and H. F. Jones, Am. J. Phys. **71**, 1095 (2003).
- [27] M. V. Berry, Proc. R. Soc. London, Ser. A **392**, 45 (1984).